

Isolation, structure elucidation, antioxidative and immunomodulatory properties of two novel dihydrocoumarins from *Aloe vera*

Xiu-feng Zhang,^{a,†} Hong-mei Wang,^{a,†} Yuan-li Song,^b Li-hua Nie,^c Lan-fen Wang,^a Bin Liu,^a Ping-ping Shen^b and Yang Liu^{a,*}

^aState Key laboratory for Structural Chemistry of Unstable and Stable Species, Center for Molecular Science, Institute of Chemistry, The Chinese Academy of Sciences, Beijing 100080, China

^bState Key Laboratory of Pharmaceutical and Biotechnology, Nanjing University, Nanjing 210008, China

^cState Key Laboratory of ChemolBiosensing and Chemometrics, Hunan University, Changsha 510008, China

Received 2 September 2005; revised 24 October 2005; accepted 28 October 2005

Available online 15 November 2005

Abstract—Two new dihydrocoumarin derivatives, compounds **1** and **2**, were isolated from *Aloe vera*. Their structures were determined by X-ray crystallographic diffraction analysis and extensive 1D, 2D NMR spectroscopic data. Both of them evidently showed antioxidant activity against superoxide and hydroxyl radicals. Only **1** obviously exhibited immunomodulatory activity in relation to increasing the phagocytic activity and stimulating the production of superoxide anions in the oxygen respiratory burst of rat peritoneal macrophages.

© 2005 Elsevier Ltd. All rights reserved.

Reactive oxygen species (ROS) play an essential role in the control of many physiological functions including the regulation of vascular tone and host immune response.¹ ROS are also usually believed to be a major damaging species involved in many pathological processes.² In general, because there is a balance between the formation and elimination of ROS in a healthy living organism, an exogenous substance that balances physiological ROS levels may be useful to maintain homeostasis.

Aloe vera has been very extensively used in health foods, cosmetics, and traditional medicines.³ Various studies have revealed that substances isolated from *Aloe* possess many pharmaceutical activities, including anti-inflammatory,⁴ anti-oxidative,⁵ anti-aged,⁶ anti-cancer,⁷ and immunomodulatory,⁸ in which the mediation of ROS levels was involved. This communication reports the isolations, structural determination and antioxidant

activity of **1** and **2** (Fig. 1), and the effect of **1** on the phagocytic activity in relation to uptaking neutral red dye and the oxygen respiratory burst of rat peritoneal macrophages.

The powdered *Aloe* sap (1000 g) was homogenized in CHCl₃, the homogenate was concentrated and dissolved in H₂O and then treated with *n*-C₆H₁₄, CHCl₃, and *n*-BuOH. Column chromatography of the CHCl₃-soluble portion (150.9 g) on silica gel and elution with solvents of increasing polarity from hexane through MeOH gave nine fractions (I–IX). Fraction (IV) was submitted to polyamides eluting with CHCl₃/CH₃COOC₂H₅ (1:1)

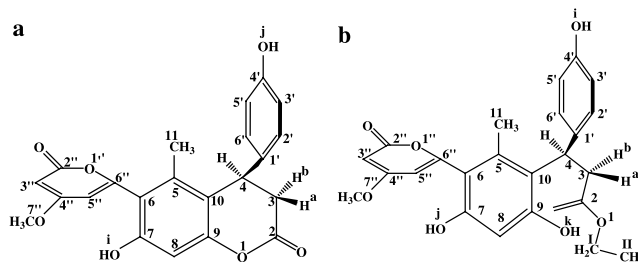


Figure 1. Molecular structures of compounds **1** (a) and **2** (b).

Keywords: *Aloe*; Dihydrocoumarins; X-ray crystallography; NMR; Antioxidant; Immunomodulatory activity.

* Corresponding author. Tel.: +86 010 62571074; fax: +86 010 82616163; e-mail: yliu@iccas.ac.cn

† These authors contributed equally to the work.

and silica gel with $n\text{-C}_6\text{H}_{14}/\text{CH}_3\text{COCH}_3$ (1:1) to yield dihydrocoumarin (**1**, 50.9 mg) and dihydrocoumarin ethyl ester (**2**, 20.5 mg).

Crystalline plates suitable for X-ray crystallographic analysis were grown in methanol solution. The crystal structures of **1** and **2** have been deposited at the Cambridge Crystallographic Data Center and allocated the deposition number CCDC: 259757 and 259758, respectively. Obviously, our X-ray result, shown as a perspective drawing of **1** and **2** in Figure 2, corresponds to the expected structure.

Compound **1** was obtained as a colorless crystal that was analyzed for $\text{C}_{22}\text{H}_{18}\text{O}_7$ by a combination of HR-FAB-MS, ^{13}C NMR spectrum, and elemental analysis data. In the IR spectrum, absorption bands at 3363.44, 1691.21, and 1639.84 cm^{-1} indicated the presence of a hydroxyl and two carbonyl groups, respectively. The ^1H NMR spectrum displays 12 different signals. A group of symmetry quartet peaks around δ 6.88 and its satellite lines represent an aromatic AA'BB' system, which can be supported further by analyzing the ^1H – ^1H COSY spectrum; A ^1H – ^1H correlation between two doublets at δ 6.22 and at δ 5.66 comes from an aromatic (pyran) ring; A singlet peak at δ 6.60 together with its correlations indicates another aromatic ring. Meanwhile, by analyzing the ^1H homonuclear decoupled and the HMQC spectra in which H-4 (δ 4.41, CH) is coupled to two individual hydrogen atoms (δ 3.20; δ 2.83), we find that the hydrogen atoms at δ 3.20 and δ 2.83 are both connected to the same carbon (C-3).

Two singlet peaks at δ 10.26 and δ 9.38 show no connectivity with any carbon nucleus in the HMQC plot, thus suggesting the existence of two hydroxyl groups. The explanation can be further supported by the disappearance of two peaks in a heavy water exchange condition. As shown in Table 1, all the chemical shifts of the protons can be easily assigned in it.

The ^{13}C NMR spectrum exhibits the presence of 20 carbon atoms whose multiplicity assignments were made by DEPT 135 and ^1H homonuclear decoupling. It clearly shows that the carbon at δ 37.74 is a $-\text{CH}_2$ group; that at δ 56.37 is a $-\text{OCH}_3$ group; that at δ 15.78 is a $-\text{CH}_3$ group. Due to overlaps of two groups of two equivalent carbons, respectively, it also indicates that two peaks at δ 115.69 and δ 127.75 represent four carbons in a *para*-substituted aromatic ring. The HMBC experiments were performed when the quaternary carbons are present (see Fig. 3). The quaternary carbon 10 is assigned as δ 115.64 from the correlations with H-8, H-11, and H-3b. Similarly, C-5, C-6, C-9, C-1', C-4', C-4'', and C-6'' are assigned as δ 136.82, δ 117.33, δ 153.13, δ 131.01, δ 156.39, δ 170.71, and δ 157.99, respectively, from the correlations between C-5 and H-4 or H-11, C-6 and H-8 or H-11, C-9 and H-4 or H-8, C-1 and H-3a, H-4 or H-3', C-4' and H-2', C-4'' and H-7'', and C-6'' and H-5''.

Compound **2** was isolated as a colorless crystal. The molecular formula $\text{C}_{22}\text{H}_{18}\text{O}_7$ was obtained by combined HR-FAB-MS and ^{13}C NMR spectrum. The spectral data of **2** were similar to those obtained for **1** (see Table 1). Significant difference in the ^1H NMR spectrum was the presence of two additional signals at δ 1.11 and δ 4.04. Correlation between methyl doublet at δ 1.11 and methylene proton at δ 4.04 was observed in the H–H COSY spectrum. These two signals gave carbon resonance in the ^{13}C NMR spectrum at δ 14.44 and δ 61.37, indicating the presence of ethoxy groups. HMBC correlation between methylene protons at δ 4.04 and carbonyl at δ 167.26 suggested the presence of an ethyl ester.

To evaluate antioxidant activity of **1** and **2** against superoxide anions and hydroxyl radicals, two assays were quantitatively examined using the ESR technology in combination with the spin trapping of 5-(diethoxy phosphoryl)-5-methyl-1-pyrroline)-*N*-oxide (DEPMPO). Superoxide anion was generated by the hypoxanthine/xanthine oxidase (XOD) system. In the presence of DEPMPO, hypoxanthine, and antioxidants, the reaction was initiated upon the addition of XOD. The characteristic signals of DEPMPO–OOH adduct ($A_N = 1.3$ 4, 1.32 mT; $A_P = 52.2$, 48.5 mT; $A_H^\beta = 11.9$, 10.3 mT and $A_H^\gamma = 0.08$ (0.043), 0.09(0.043) mT) were obviously observed in the presence and in the absence of the compound. Generation of hydroxyl radical was performed in Fenton's mixture that was composed of ferrous ion, EDTA, and hydroxyl peroxide. When spin trap DEPMPO is presented, the octet ESR peaks can be obtained under Fenton's conditions. The signal indicates the hyperfine splittings characteristic for DEPMPO–OH adduct ($A_N = 1.40$ mT; $A_P = 4.74$ mT; $A_H^\beta = 1.30$ mT and $A_H^\gamma = 0.027$ mT). The supplementation of **1** and **2**

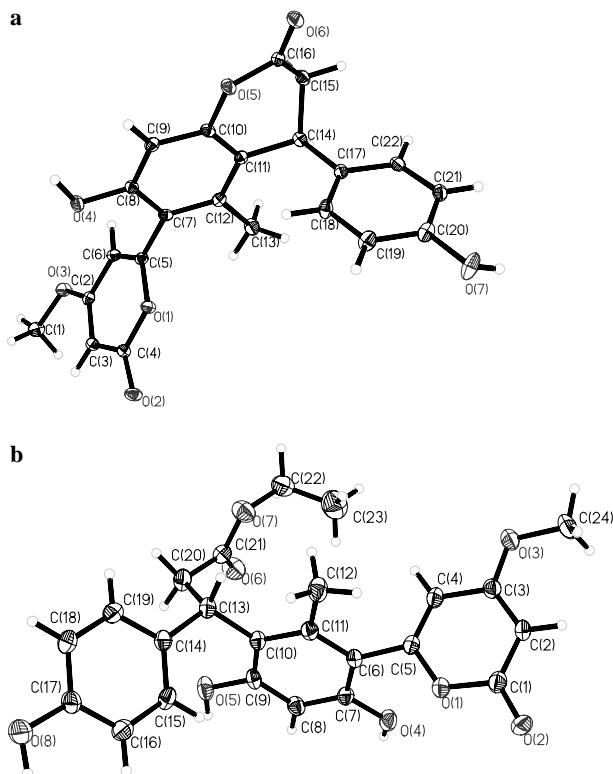
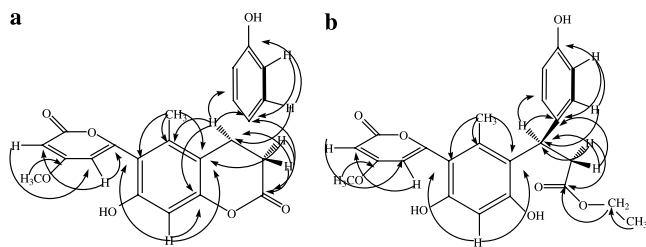


Figure 2. ORTEP plot and numbering of compound **1** (a) and **2** (b).

Table 1. Summary of NMR data for compound **1** (in DMSO-*d*₆) and compound **2** (in methanol-*d*₃)

Position	¹ H (δ, ppm)		¹³ C (δ, ppm)		HMBC correlations	
	Compound 1	Compound 2	Compound 1	Compound 2	Compound 1	Compound 2
2			175.20	167.26		
3	a.3.21 (m) b.2.83 (m)	a.3.30 (m) b.3.18 (m)	39.50	37.74	C-4, 2, 1' C-10, 2	C-4,1' C-10, 2
4	4.41 (d,5.86)	4.80 (t,3.26)	39.40	36.08	C-1'2'5,9	C-1'2'
5			139.09	136.82		
6			121.79	117.33		
7			159.70	155.67		
8	6.60 (s)	6.60 (s)	101.97	101.54	C-9,10,6	C-10,6
9			156.29	153.13		
10			114.01	115.64		
11	1.97 (s)	2.15 (s)	17.88	15.78	C-5,10,6	C-5,10,6
1'			135.72	131.01		
2'	6.86 (d,8.53)	7.07 (d,8.52)	129.41	127.75	C-4, 4'	C-4, 4'
3'	6.70 (d,8.53)	6.70 (d,8.62)	115.69	115.69	C-1'	C-1'
4'			156.15	156.39		
2''			168.59	163.82		
3''	5.66 (d,2.15)	5.61 (d,2.22)	88.59	88.27	C-5''	C-5''
4''			173.89	170.71		
5''	6.22 (d,2.15)	6.11 (d,2.22)	106.53	104.41	C-6'', 3''	C-3''
6''			161.88	157.99		
7''	3.84 (s)	3.88 (s)	56.90	56.37	C-4''	C-4''
I		4.04 (q,7.24)		61.37		C-2...
II		1.11 (t,7.18)		14.44		C-1

**Figure 3.** Key HMBC correlations of compounds **1** (a) and **2** (b).

significantly scavenges the production of both radicals, the percentage inhibitions of superoxide ion and hydroxyl radical are 29.83% and 43.67% by **1** and 30.33% and 42.33% by **2**, respectively. The observations clearly indicate that two dihydrocoumarins have similar antioxidant capacity, structurally to say, because both of them have a uniform aromatic skeleton together with the same hydroxyl substitutions, except that there exists a hydroxyl group in site **k** of **2**.

The phenolic compounds can scavenge the hydroxyl radical by a hydrogen abstraction occurring on the hydroxyl groups. Theoretically to say, the free radical scavenging activity of the two compounds can be characterized by the O–H bond dissociation enthalpy (BDE) to a certain extent.⁹ To ascertain the active center for the H-abstraction, we accordingly calculated the O–H BDE values by the B3LYP/6-31G (P)/AM1/AM1 method ($\text{O–H BDE} = H_f + H_h - H_p$, in which, H_f is the enthalpy of phenoxy radical generated after H-abstraction, H_h represents the enthalpy of hydrogen, and H_p the enthalpy of phenol). The solvent (H_2O) effect was taken into consideration in all of the calculations by employing the self-consistent reaction field (SCRF) method with polarized continuum model (PCM). The lower the calculated O–H BDE is, the more active this

site is. As calculated from **1**, the O–H BDEs of the hydroxyl in site **i** and site **j** are 100.42 and 127.38 kcal/mol, respectively, site **i** is therefore more reactive than site **j**. Regarding the calculation of **2**, the O–H BDE of the hydroxyl in site **i** (85.50 kcal/mol) is lower than those in site **j** (87.02 kcal/mol) and site **k** (105.78 kcal/mol). Like in **1**, site **i** in **2** also can be ascertained as an active position, accordingly. The similarity of two compounds in the H-abstraction by hydroxyl radical probably results in a similar percentage inhibition.

Immunomodulatory activity of **1** and **2** was examined by stimulating the phagocytic capacity and the oxygen respiratory burst of the rat peritoneal macrophages. Peritoneal macrophages were isolated from rat and grown in RPMI-1640 medium supplemented with 10% heat-inactivated fetal bovine serum in 96-well chamber slides. To evaluate the effects of the two compounds on phagocytic capacity, we preincubated macrophages with **1** or **2** at a concentration of 25, 50, 100, and 200 μM . Lipopolysaccharide (LPS; Sigma) at 5 $\mu\text{g}/\text{ml}$ was used as a positive control and medium only as a negative control. After 12 h incubations, the medium was removed and washed twice in PBS. 100 μl of Hanks and 100 μl neutral red solution at 0.0072 mg/ml were added into each well. After 30 min incubations, the medium was removed and washed twice in PBS, 200 μl phagocytolytic liquid was added into each well, and the absorbance was measured at 540 nm using a UV-spectrophotometer. The capacity of macrophages for uptaking neutral red is comparatively illustrated in Figure 4. It is clearly indicated that the phagocytotic function of macrophages was significantly and dose-dependently increased by **1** at concentrations of 50–200 $\mu\text{g}/\text{ml}$, but **2** showed no effect. The increase obtained with **1** at the maximum concentration tested (200 μM) was even higher than that obtained from the positive control.

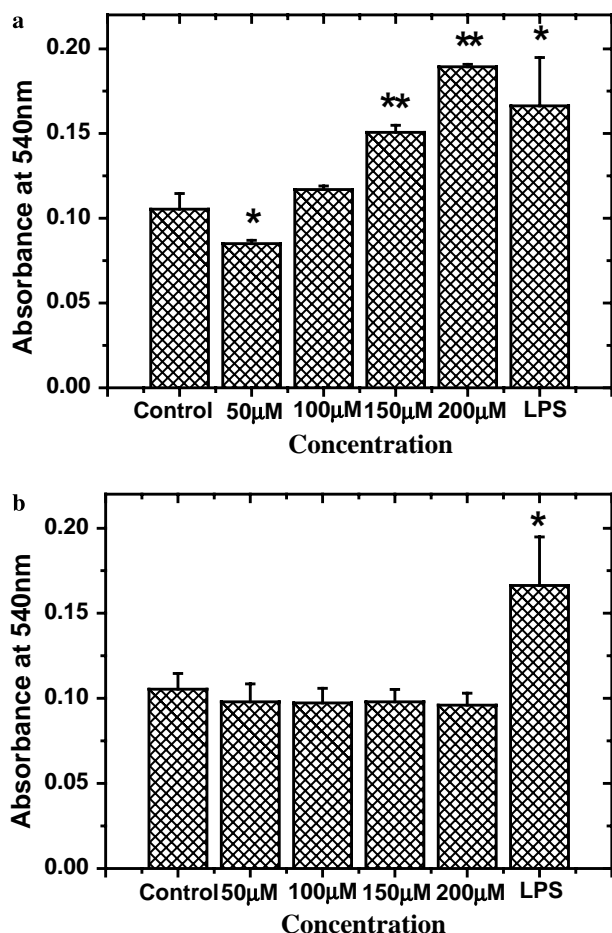


Figure 4. Effects of compounds **1** (a) and **2** (b) on the phagocytotic function of peritoneal macrophages. Values shown are means ($n = 3$) \pm standard errors. Significant differences with control group (macrophages incubated in the absence of compounds) were designated as * $P < 0.05$, ** $P < 0.01$.

To examine the effects of two compounds on PMA-stimulated $O_2^{\cdot-}$ production in the respiratory burst of rat peritoneal macrophages, cells were incubated with **1** or **2** at a concentration of 200 μ M. Control experiment was performed simultaneously without drug incubation. After 12 h incubation, the medium was removed and washed twice in PBS. RPMI 1640 medium (37.5 μ l), 50 μ l DATAPAC, 62.5 μ l of 0.2 mM DEPMPO, and 100 μ l PMA (100 ng/ml) were successively added to each well and incubated with the cells for 5 min in a culture chamber. The ESR spectra obtained from the trapped DEPMPO–OOH adduct were collected on a Bruker ESP 300 spectrometer, as illustrated in Figure 5. Twelve hours preincubation of **1**, but not for **2**, resulted in an enhancement of the respiratory burst of the macrophages. In order to avoid a direct scavenging on superoxide anion during the respiratory burst by the dihydrocoumarins themselves, PBS twice-repeatedly washed the incubated macrophages before the PMA-stimulated respiratory burst was initiated. Accordingly, we can separately demonstrate their enhancing PMA-stimulated respiratory burst and scavenging superoxide anion.

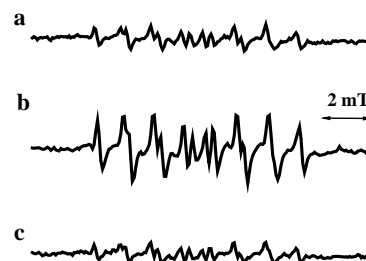


Figure 5. Effects of compounds **1** and **2** on the superoxide production initiated by PMA-simulated oxidative respiratory burst of peritoneal macrophages. (a) ESR spectrum obtained in the absence of title compounds; (b) pre-incubated by **1** for 12 h; (c) pre-incubated by **2** for 12 h.

Macrophages play a significant role in the host defense mechanism. When activated they inhibit the growth of a wide variety of tumor cells and microorganisms. Macrophages generate large quantities of ROS, including superoxide anion and nitric oxide, in response to a variety of membrane stimulants, by a coordinated sequence of biochemical reactions known as the oxidative burst.¹⁰ The superoxide anion and nitric oxide released from respiratory burst response of macrophages can kill invading pathogen or cancer cells in immune response, although overproduction of both radicals may introduce oxidative stress on normal cells and be implicated in many pathological processes. The above observations indicate that only **1** is a good stimulator for the phagocytic process and the respiratory burst.

Comparison of the molecular structures of **1** and **2** shows that the only difference for the two compounds is located in the benzopyrone ring. Instead of a lactone ring in **1**, an open ring acetic ester exists in **2**. Obviously, it is the pivotal close lactone ring in **1** that plays an essential role in stimulating the immunomodulatory activities in relation to phagocytic activity and oxygen respiratory burst. More importantly, it is only **1** that seems to be beneficial in regulating the ROS levels by directly scavenging ROS and promoting the oxygen respiratory burst, and therefore, to be useful in the potential application as a candidate of immunomodulatory drug on the immune system.

Acknowledgments

We are grateful to the NSFC (No. 30128003), the Outstanding Overseas Chinese Scholars Fund of Chinese Academy of Sciences (2005-1-12), and State Key Laboratory of Chemo/Biosensing and Chemometrics for financial support.

References and notes

- (a) Furchgott, T. F.; Zawadzki, J. V. *Nature* **1980**, 288, 373; (b) Babior, B. M.; Kipnes, R. S.; Curnutte, J. T. *J. Clin. Invest.* **1973**, 52, 741.
- (a) Finkel, T.; Helbrook, N. J. *Nature* **2000**, 408, 239; (b) Beckman, K. B.; Ames, B. N. *Physiol. Rev.* **1998**, 78, 547;

- (c) Xia, Y.; Khatchikian, G.; Zweier, J. L. *J. Biol. Chem.* **1996**, *271*, 10096.
3. (a) Reynolds, T. *Bot. J. Linn. Soc.* **1985**, *90*, 157; (b) Grindlay, D.; Reynolds, T. *J. Ethnopharmacol.* **1986**, *16*, 117.
4. Yagi, A.; Kabash, A.; Okamura, N.; Haraguchi, H.; Moustafa, S. M.; Khalifa, T. I. *Planta Med.* **2002**, *68*, 957.
5. (a) Yagi, A.; Kabash, A.; Mizuno, K.; Moustafa, S. M.; Khalifa, T. I.; Tsuji, H. *Planta Med.* **2003**, *69*, 269; (b) Vargas, F. R.; Diaz, Y. H.; Carbonell, K. M. *Pharm. Biol.* **2004**, *42*, 342.
6. Lim, B. O.; Seong, N. S.; Choue, R. W.; Kim, J. D.; Kim, J. D.; Lee, H. Y.; Kim, S. Y.; Yu, B. P.; Jeon, T. I.; Park, D. K. *J. Nutr. Sci. Vitaminol.* **2003**, *49*, 292.
7. (a) Su, Y.-T.; Chang, H.-L.; Shyue, S.-K.; Hsu, S.-L. *Biochem. Pharmacol.* **2005**, *70*, 229; (b) Desai, K. N.; Wei, H.; Lamartiniere, C. A. *Cancer Lett.* **1996**, *101*, 93.
8. (a) Im, S. A.; Oh, S. T.; Song, S.; Kim, D. S.; Woo, S. S.; Jo, T. H.; Park, Y. I.; Lee, C. K. *Int. Immunopharmacol.* **2005**, *5*, 271; (b) Karaca, K.; Sharma, J. M.; Nordgren, R. *Int. J. Immunopharmacol.* **1995**, *17*, 183; (c) Sjeraba, A.; Quere, P. *Int. J. Immunopharmacol.* **2000**, *22*, 365; (d) Lee, J. K.; Lee, M. K.; Yun, Y. P.; Kim, J. S., et al. *Int. Immunopharmacol.* **2000**, *1*, 1275.
9. (a) Migliavacca, E.; Carrupt, P. A.; Testa, B. *Helv. Chim. Acta* **1997**, *80*, 1613; (b) Zhang, H. Y. *J. Am. Oil Chem. Soc.* **1998**, *75*, 1705; (c) Van Acker, S. A. B. E.; Koymans, L. M. H.; Bast, A. *Free Radical Biol. Med.* **1993**, *15*, 311.
10. Mauél, J. *Adv. Parasitol.* **1996**, *28*, 1.